Kinetic and thermodynamics studies on the decompositions of Ni₃C in different atmospheres

Yonghua Leng[a], Lei Xie[a], Fuhui Liao[a], Jie Zheng[a], Xingguo Li[a,b,*]

[a] *Beijing National Laboratory for Molecular Sciences (BNLMS), The State Key Laboratory of Rare Earth Materials Chemistry and Applications, College of Chemistry and Molecular Engineering, Peking University, Beijing 100871, China*
[b] *College of Engineering, Peking University, Beijing 100871, China*

ARTICLE INFO

ABSTRACT

The thermal decompositions (including TG and DSC) of nickel carbide were studied under different atmospheres of Ar, air and H_2. X-ray diffraction combined with element analysis indicated that nickel metal, together with solid amorphous carbon, was formed during Ni_3C decomposition in Ar atmosphere, accompanying mass invariant in this process. While in H_2 atmosphere nickel metal was the only residual from reactions. The carbon component of nickel carbide reacted with H_2 to form methane as the main volatile gases. Both the nickel and carbon components of Ni_3C reacted with O_2 in the air to form their corresponding oxides. Moreover, we calculated the activation energy for the decomposition process and the molar enthalpy of formation of Ni_3C based on the thermal analysis.

© 2008 Elsevier B.V. All rights reserved.

1. Introduction

Ni_3C has a metastable phase at room temperature and decomposes at the temperatures above 430 °C in inert atmosphere, which make it hard to be synthesized [1]. Although many literatures have reported the formation of thin Ni_3C film [2,3], in the case of pure Ni_3C powder, only few groups succeeded to convert nickel metal fully into Ni_3C phase [4,5]. As a metastable phase resulted from the low solubility of carbon into nickel at high temperature and lack of ionic bonding [6], however, no detailed study has been reported on the decomposition of Ni_3C.

Synthesis of pure Ni_3C powder becomes the key to study the thermodynamics of Ni_3C and calculate its kinetic parameters. Recently, our group reported that pure Ni_3C powder could be transformed from Ni nanoparticles in organic solutions in the presence of surfactants [7], which provide us the possibility to study the thermal stability of Ni_3C phase. In addition, it is hard to distinguish hexagonal-close-packed Ni metal (JCPDS 45-1027) from Ni_3C phase (JCPDS 06-0697) according to their XRD patterns [8–10]. By analyzing the decomposition products, it may offer us an effective way to distinguish these two materials. In this paper, we reported the decomposition of Ni_3C phase in different atmospheres, including the inert argon, the oxidative air and the reductive hydrogen. The activation energies and the molar enthalpy of formation of Ni_3C were also calculated based on the thermal analysis.

2. Experimental

Well-characterized Ni_3C nanoparticles were prepared in 1-octadecene by the decomposition of nickel formate, according to a slightly modified procedure reported by our group [7]. The nanoparticles were found to consist of pure Ni_3C phase, which was used for further decomposition in different atmospheres.

Thermogravimetric and differential scanning calorimetric (TG–DSC, NETZSCH STA 449 C) curves were recorded at 10 K/min in Ar (99.99%), H_2 (99.99%) and air atmospheres. Highly sintered α-Al_2O_3 was used as a reference material for the thermal measurements. This thermal analyzer is equipped with a mass spectrometer (MS) to detect the volatile components during the decomposition process. During the measurements, the sample mass was ca. 10 mg and all runs were conducted at a gas flow rate of 40 mL min^{-1}. In order to calculate the activation energy for the reaction of Ni_3C under different atmospheres, heating rates were varied 5, 10 and 20 K/min, respectively. X-ray diffraction (XRD, RIGAKU D/MAX-2400) was conducted using Cu Kα radiation to identify their structure of the decomposition solid products. 2θ scans were made from 30° to 80° at a rate of 4°/min with a step size of 0.02°. The

* Corresponding author at: Beijing National Laboratory for Molecular Sciences (BNLMS), The State Key Laboratory of Rare Earth Materials Chemistry and Applications, College of Chemistry and Molecular Engineering, Peking University, Beijing 100871, China. Tel.: +86 10 6276 5930; fax: +86 10 6276 5930.
E-mail address: xgli@pku.edu.cn (X. Li).

measurements were conducted using a generator voltage of 40 kV and a current of 100 mA. Microscale elements analysis instrument (ELEMENTAR Vario EL) was adopted to detect the carbon content in the decomposed products using combustion analysis.

3. Results and discussion

3.1. Ni₃C decomposition in Ar atmosphere

Fig. 1 shows TG, DSC and MS curves of Ni₃C decomposition in Ar atmosphere at a heating rate of 10 K/min. The curves indicate that Ni₃C decomposes via a weight-loss step (process I) maximized at 540 K, ending up with solid products that produces an exothermic peak centered around 688.2 K (process II). In process I, the endothermic peak is attributed to the decomposition of the adsorbed surfactants on the surface of the Ni₃C particles. MS data identified the formation of small fractions of C, CO, CO_2, O, OH and H_2O during this process, corresponding to the mass loss by 2.9 wt% from 500 to 570 K in the TG curve. There is also an exothermic peak at 688.2 K in process II, which is associated to the decomposition of Ni₃C. The temperature for Ni₃C to decompose is slightly lower than that previously reported result, which is above 430 °C (703 K) [1]. Since no mass loss during process II is observed in the TG curve and no volatile gases are detected by MS, this process could be assigned to either a physical process, i.e. recrystallization of a solid product, or a decomposition process, during which all the decomposition products are solid matter. The decomposition products will be validated below in detail.

The as-synthesized Ni₃C nanoparticles was heated to 600 K at a heating rate of 10 K/min and then cooled to room temperature, that is, after the endothermic peak is completed (process I), but before the emergence of the exothermic peak (process II), the decomposed product was measured with XRD. As shown in Fig. 2(b), no structural change was observed compared with the XRD pattern of the as-synthesized Ni₃C (Fig. 2(a)), which confirms that the endothermic peak belongs to the decomposition and desorption of the adsorbed surfactants. This result agrees well with the MS data by detecting the small molecules coming from the surfactants (process I). According to the Scherrer equation, the average crystallite size of Ni₃C was estimated to be 40 nm, which was slight smaller than that calculated from the TEM image (supporting information). Microscale element analysis by combustion experiment confirms
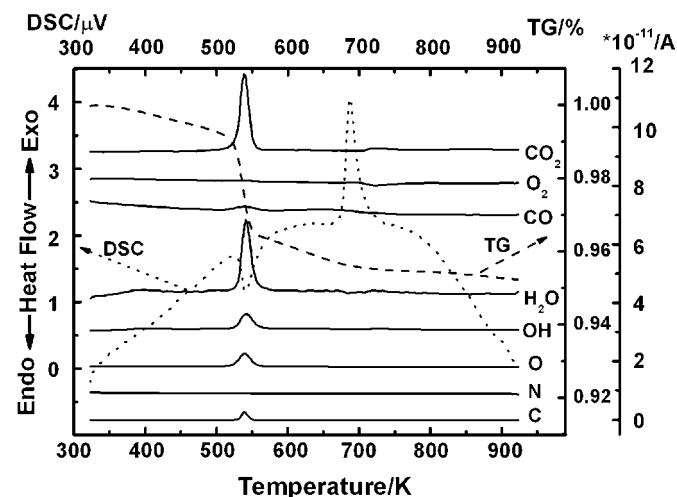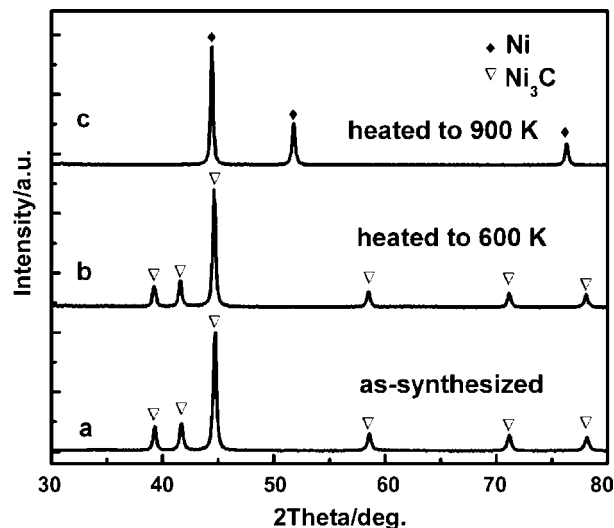

Fig. 2. XRD patterns for: (a) the as-synthesized Ni₃C nanoparticles, (b) the powders obtained after heating to 600 K in Ar and (c) the powders obtained after heating to 900 K in Ar.

that the carbon content is 6.42 wt% in the product after heating to 600 K, which accords well with the value of 6.38 wt% for pure Ni₃C phase. This result implies that after heating to 600 K, the product changes to pure Ni₃C with clean surfaces. After heating to 900 K, Ni₃C nanoparticles decompose to produce nickel metal (JCPDS 04-0850), as shown in Fig. 2(c), indicating that the exothermic peak was owing to the Ni₃C decomposition. Because no mass loss was observed in TG curves, no volatile carbon detected by MS and no crystalline carbon observed from XRD pattern during process II, microscale element analysis was performed to validate the presence of carbon in the decomposition products. It indicates that 6.39 wt% of carbon in the decomposed product after heating to 900 K, agreeing well with the carbon content in Ni₃C. This result confirms that the hcp phase should be Ni₃C rather than hcp Ni metal. Though such a large quantity of solid carbon was formed in this process, no crystalline carbon was detected by XRD, suggesting the carbon coexists with nickel metal in an amorphous state. The decomposition equation for Ni₃C in Ar atmosphere should be

$$Ni_3C(s) = 3Ni(s) + C(s, \text{amorphous}) \tag{1}$$
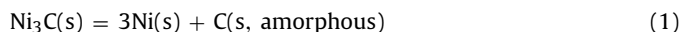
The decomposition of Ni₃C in Ar was identified to be a single step reaction. In this case, the activation energy ΔE could be calculated for the decomposition process using Kissinger method based on the following equation [11]:

$$\ln\left(\frac{C}{T_p^2}\right) = -\left(\frac{\Delta E}{K_B T_p}\right) + A \tag{2}$$

where C is the heating rate, ΔE the activation energy, T_p the peak temperature, K_B Boltzmann constant, and A is a constant. With increasing heating rate, the peaks shift to higher temperatures. From the peak shift, ΔE could be calculated. As shown in Fig. 3, when the heating rates increase from 5 to 10 K/min and 20 K/min in Ar atmosphere, the peak temperature is 673.3, 688.2 and 698.0 K, respectively. According to Eq. (2), the calculated ΔE for Eq. (1) is 204 kJ mol⁻¹, with a correlation coefficient r to be 0.991.

DSC measurements are also used to calculate some thermodynamics parameters. The enthalpy (ΔH, J g⁻¹) of the thermal events could be directly determined from the DSC data (recorded at 10 K/min) according to the peak area. The determined ΔH is used to calculate the specific heat capacity (C_p, J K⁻¹ g⁻¹) using the equation of $C_p = \Delta H/\Delta T$, where $\Delta T = T_2 - T_1$, and T_1 is the temperature from

Fig. 1. TG, DSC and MS curves recorded for Ni₃C at 10 K/min in a dynamic atmosphere of Ar (the dash line denotes the TG curve, the short-dash line denotes the DSC curve and the solid lines denote the MS data).
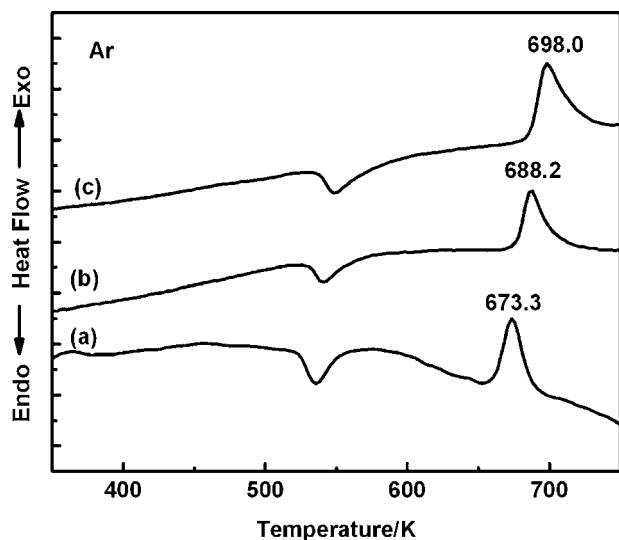
Fig. 3. DSC curves recorded for Ni_3C decomposing at various heating rates in Ar: (a) 5 K/min, (b) 10 K/min and (c) 20 K/min.

Table 1
Thermodynamic parameters for the decomposition of Ni_3C in Ar atmosphere

ΔH (J g^{-1})	140.5
C_p (J K^{-1} g^{-1})	6.4
ΔS (J K^{-1} g^{-1})	0.2

which the DSC curve begins to depart from the base line, while T_2 is the temperature at which the peak lands. Then using the equation of $\Delta S = 2.303 C_p \log(T_2/T_1)$, the entropy change ($\Delta S$, J K^{-1} g^{-1}) could be obtained [12]. From the DSC curves measured at the heating rate of 10 K/min in Ar atmosphere, the thermodynamic parameters were listed in Table 1. The molar enthalpy of formation ($\Delta_f H$) for Ni_3C is calculated to be 26.4 kJ mol^{-1} ($M_w \times \Delta H$, M_w is the molecular weight of Ni_3C).

3.2. Ni_3C decomposition in H_2

To eliminate the influence of surfactants, Ni_3C powder was pre-heated to 600 K at a heating rate of 10 K/min in Ar and then cooled to room temperature before decomposition under air and H_2 atmospheres. TG and MS curves for Ni_3C decomposition in H_2 at a heating rate of 10 K/min are shown in Fig. 4. Ni_3C powder decomposes in
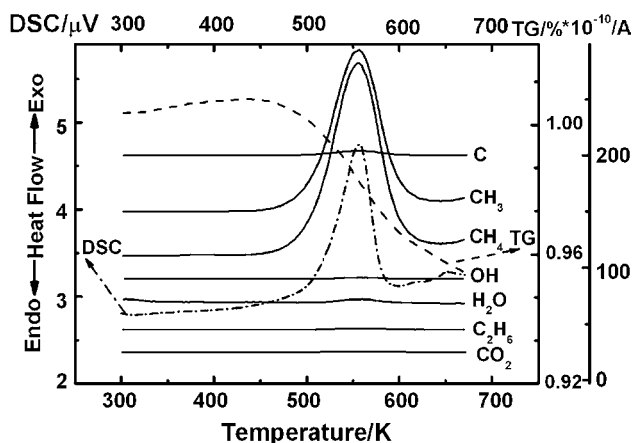

Fig. 4. TG, DSC and MS curves recorded for Ni_3C at 10 K/min in a dynamic atmosphere of H_2.
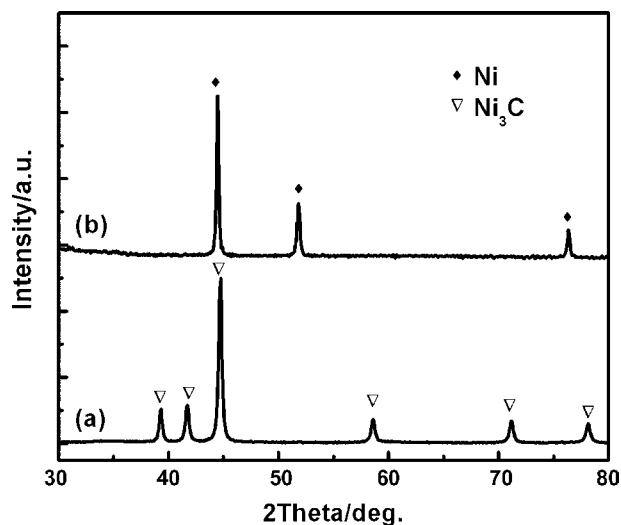

Fig. 5. XRD patterns for: (a) the as-synthesized Ni_3C nanoparticles; (b) the powders obtained after decomposing in H_2 at 673 K.

H_2 via a weight-loss process. Meanwhile, volatile hydrocarbons are formed, which are taken away by the flowing H_2. The release of carbon component from Ni_3C powder results in the loss of weight. The MS data indicates that the hydrocarbon gases comprise mainly methane and small amount of ethane. Though the XRD pattern for the decomposition product of Ni_3C at 673 K in H_2 (Fig. 5(b)) is similar to that in Ar (Fig. 2(c)), only negligible amount of carbon is detected in the decomposed product by microscale element analysis, indicating nickel metal the only residue after decomposition.

Distinct from the Ar gas just as a purge and protective gas, H_2 participates in the reaction of Ni_3C decomposition, which combines the carbon component in Ni_3C and forms volatile hydrocarbon. For the multistep nature of solid state reaction, here isoconversional method was used to calculate the activation energy [13,14], where the activation energy showed dependence on experimental conditions, such as the extent of conversion, sample mass and the temperature and so on. In the case of nickel carbides in H_2, the activation energy was calculated from the TG curves at different heating rates according to the Ozawa–Wall–Flynn equation [15]:

$$\log \beta = 0.4567 \left(\frac{\Delta E}{R} \right) \left(\frac{1}{T} \right) + A$$

where β is the heating rate, ΔE the activation energy, T the absolute temperature and R is the gas constant. Fig. 6 shows the relationship between the heating rate and reciprocal absolute temperature. It is apparent that the gradient for several lines under different reaction conversion is identical within error. The apparent activation energy ΔE as a function of conversion degree was shown in Table 2.

For the thermal decomposition of Ni_3C in H_2, the activation energy increased a little when the extent of conversion not more than 0.4.

The participation of H_2 in the reaction accelerates the decomposition process and decreases the decomposition temperature

Table 2
The apparent activation energy as a function of conversion degree (α)

$1 - \alpha$	E (kJ mol^{-1})
0.9	71.3
0.8	75.7
0.7	76.9
0.6	78.2
0.5	77.4
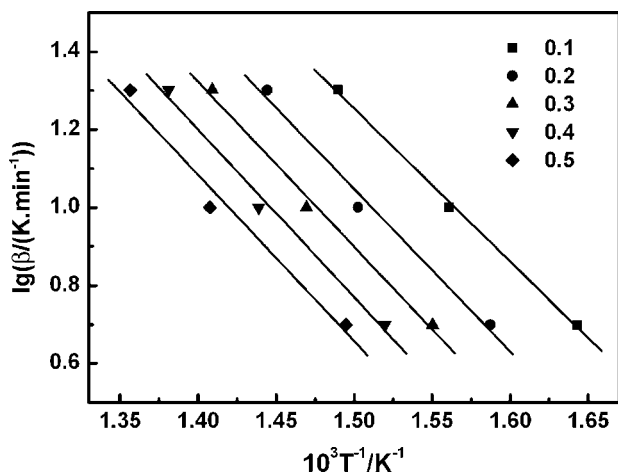
Fig. 6. Isoconversional plots of Ni_3C reacted in H_2 with different conversion degrees.

Fig. 8. XRD patterns for the powder obtained after Ni_3C was heated to 823 K in the air at various heating rates (a) 5 K/min, (b) 10 K/min and (c) 20 K/min.

dramatically. The decomposition equation for Ni_3C in H_2 is

$$Ni_3C(s) + 2H_2(g) = 3Ni(s) + C_xH_y(g) \qquad (3)$$

3.3. Ni_3C decomposition in air

Ni_3C powder was also pre-treated in Ar atmosphere to eliminate the surfactants before decomposing in the air. Fig. 7 shows the TG, DSC and MS curves of Ni_3C decomposing in the air. Oxygen participates in the reaction, as indicated by the decrease of the O_2 amount. Thus to be more precise, in this case it is not a decomposition, but oxidation of Ni_3C instead. Though accompanied the release of carbon from Ni_3C to form dioxide, the TG curve underwent a wide weight-increased process from 550 to 740 K for the nickel component reacted with oxygen to produce NiO (Fig. 8) and caused a net mass increase in the solid product. The DSC curve which was composed of three peaks seems a little complicated, which is somewhat similar to the MS information of CO_2. Shimada reported that oxidation of the metal component in the carbides for MC (M = Zr, Ti and Hf) prior to that of the carbon component though the proceeding oxidation of M with subsequent oxidation of carbon was also similarly observed [16]. As a result, exceeding 100% oxidation was
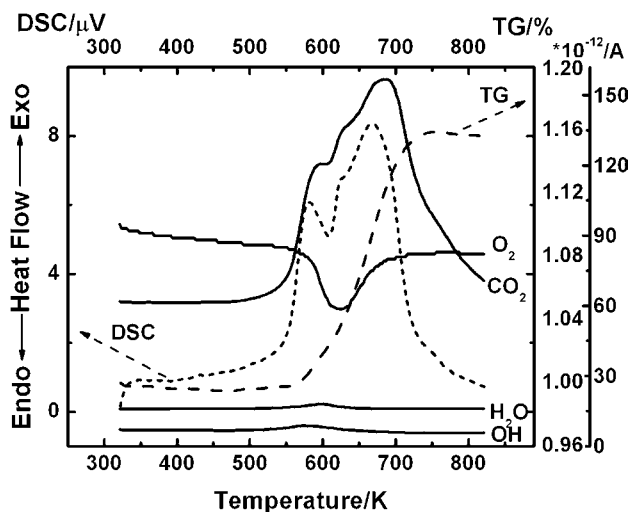
obtained due to the retention of carbon according to the following equation

$$MC + O_2 = MO_2 + C$$
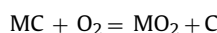
However, for our Ni_3C sample, the case was quite different. Considering the formation of CO_2 throughout the whole process of weight increase caused by the formation of NiO, the oxidative reactions for the carbon and nickel component with O_2 take place at the same time. We could not observe a clear gap between the oxidation of nickel and the oxidation of carbon component. This chemical phenomenon indicates the overlapping reaction of both nickel and carbon components in Ni_3C with O_2. The complexity of the DSC peaks and detectable nickel metal in the decomposed product (Fig. 8) hinder us to calculate the activated energy. The difference in the oxidation of Ni_3C and ZrC may result from the metastable properties of Ni_3C. Also, the nano-scale particles may be responsible for the high activity of carbon in Ni_3C, leading to the oxidation reaction for carbon occur together with the metal oxidation. At least three exothermic peaks were observed, which may attribute to the release of CO_2 based on the almost identical shapes of DSC curve and the MS for CO_2. This phenomenon could be explained by the high surface area of our sample. The small particle size (Figure S1) favored adsorption of the gaseous decomposition products. As a result, the exothermic decomposition was controlled by mass-transfer and desorption along the solid surface, which are usually characterized by relatively low activation energies. Although we could not estimate the activation energy of Ni_3C decomposition in the air, the low activation energy for Ni_3C decomposing in Ar and H_2 could testify that the high surface area played a crucial role in the reaction.

4. Conclusions

In summary, the decomposition of Ni_3C in Ar, H_2 and air were studied. Decomposition in Ar is a single-step reaction with activation energy of 204 kJ mol^{-1}, yielding Ni metal and amorphous carbon. Decomposition in H_2 to give Ni and hydrocarbon has much lower activation energy depending on the conversion degree. Reaction with oxygen in the air shows a complicated exothermal peak, without any clear indication of the sequence oxidation of the two components.

Fig. 7. TG, DSC and MS curves recorded for Ni_3C decomposing at 10 K/min in an oxidative atmosphere of air (the dash line denotes the TG curve, the short-dash line denotes the DSC curve and the solid lines denote the MS data).
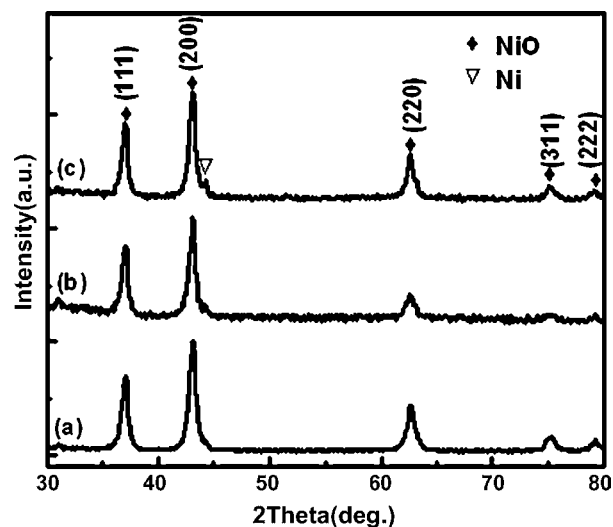
Acknowledgements

Appendix A. Supplementary data

Supplementary data associated with this article can be found, in the online version, at doi:10.1016/j.tca.2008.04.003.

References

[1] D.L. Leslie-Pelecky, X.Q. Zhang, S.H. Kim, M. Bonder, R.D. Rieke, Chem. Mater. 10 (1998) 164–171.
[2] S. Sinharoy, L.L. Levenson, Thin Solid Films 53 (1978) 31–36.
[3] S. Sinharoy, M.A. Smith, L.L. Levenson, Surf. Sci. 72 (1978) 710–718.
[4] K. Tokumitsu, Mater. Sci. Forum 235 (1997) 127–132.
[5] P. Hooker, J.T. Beng, K.J. Klabunde, S. Suib, Chem. Mater. 3 (1991) 947–952.
[6] L.P. Yue, R. Sabiryanov, E.M. Kirkpatrick, D.L. Leslie-Pelecky, Phys. Rev. B 62 (2000) 8969–8975.
[7] Y.G. Leng, H.Y. Shao, Y.T. Wang, M. Suzuki, X.G. Li, J. Nanosci. Nanotechnol. 6 (2006) 221–226.
[8] V. Tzitzios, G. Basina, M. Gjoka, V. Alexandrakis, V. Georgakilas, D. Niarchos, N. Boukos, D. Petridis, Nanotechnology 17 (2006) 3750–3755.
[9] Y.T. Jeon, J.Y. Moon, G.H. Lee, J. Park, Y. Chang, J. Phys. Chem. B 110 (2006) 1187–1191.
[10] M. Richard-Plouet, M. Guillot, S. Vilminot, C. Leuvrey, C. Estournes, M. Kurmoo, Chem. Mater. 19 (2007) 865–871.
[11] H.E. Kissinger, Anal. Chem. 29 (1957) 1702–1706.
[12] M.A. Mohamed, S.A.A. Mansour, M.I. Zaki, Thermochim. Acta 138 (1989) 309–317.
[13] S. Vyazovkin, Int. Rev. Phys. Chem. 19 (2000) 45–60.
[14] S. Vyazovkin, New J. Chem. 24 (2000) 913–917.
[15] T. Ozawa, Bull. Chem. Soc. Jpn. 38 (1965) 1881–1886.
[16] S. Shimada, Solid State Ionics 141–142 (2001) 99–104.